Cell Insight 1 (2022) 100005

Contents lists available at ScienceDirect

Cell Insight

journal homepage: www.journals.elsevier.com/cell-insight

Full Length Article

Single-cell transcriptomic landscape identifies the expansion of peripheral blood monocytes as an indicator of HIV-1-TB co-infection

Qinglong Guo [a,1], Yu Zhong [b,1], Zhifeng Wang [b,1], Tingzhi Cao [a,1], Mingyuan Zhang [b], Peiyan Zhang [a], Waidong Huang [b,c], Jing Bi [a], Yue Yuan [b,c], Min Ou [a], Xuanxuan Zou [b,c], Guohui Xiao [a], Yuan Yang [b], Shiping Liu [b,d], Longqi Liu [b], Zhaoqin Wang [a], Guoliang Zhang [a,*], Liang Wu [b,d,**]

[a] *National Clinical Research Center for Infectious Diseases, Guangdong Provincial Clinical Research Center for Tuberculosis, Shenzhen Third People's Hospital, Southern University of Science and Technology, Shenzhen, 518112, China*
[b] *BGI-Shenzhen, Beishan Industrial Zone, Shenzhen, 518083, China*
[c] *College of Life Sciences, University of Chinese Academy of Sciences, Beijing, 100049, China*
[d] *Shenzhen Key Laboratory of Single-cell Omics, BGI-Shenzhen, Shenzhen, 518100, China*

HIGHLIGHTS

- PBMC scRNA-seq performed on patients with HIV-1 alone and HIV-1-TB co-infection.
- Immune dysregulation corresponds to different disease states (HIV/HIV-1-TB).
- An inflammatory $CD14^{+}CD16^{+}$ monocyte subset elevated in HIV-pre & TB-pre group.
- Monocyte subsets can distinguish HIV-1-TB co-infection from HIV-pre group.

GRAPHICAL ABSTRACT

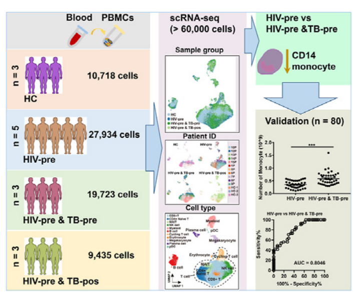

ARTICLE INFO

Keywords:
Single-cell RNA sequencing
Peripheral blood mononuclear cells
HIV-1-TB co-infection
$CD14^{+}CD16^{+}$ monocytes

ABSTRACT

Certain circulating cell subsets are involved in immune dysregulation in human immunodeficiency virus type 1 (HIV-1) and tuberculosis (TB) co-infection; however, the characteristics and role of these subclusters are unknown. Peripheral blood mononuclear cells (PBMCs) of patients with HIV-1 infection alone (HIV-pre) and those with HIV-1-TB co-infection without anti-TB treatment (HIV-pre & TB-pre) and with anti-TB treatment for 2 weeks (HIV-pre & TB-pos) were subjected to single-cell RNA sequencing (scRNA-seq) to characterize the transcriptome of different immune cell subclusters. We obtained > 60,000 cells and identified 32 cell subclusters based on gene expression. The proportion of immune-cell subclusters was altered in HIV-1-TB co-infected individuals compared with that in HIV-pre-group, indicating immune dysregulation corresponding to different disease states. The proportion of an inflammatory $CD14^{+}CD16^{+}$ monocyte subset was higher in the HIV-pre & TB-pre group than in the HIV-pre group; this was validated in an additional cohort ($n = 80$) via a blood cell differential test, which also demonstrated a good discriminative performance (area under the curve, 0.8046). These findings depicted the

* Corresponding author. National Clinical Research Center for Infectious Diseases, Guangdong Provincial Clinical Research Center for Tuberculosis, Shenzhen Third People's Hospital, Southern University of Science and Technology, Shenzhen, 518112, China.

** Corresponding author. BGI-Shenzhen, Beishan Industrial Zone, Shenzhen, 518083, China.

E-mail addresses: szdsyy@aliyun.com (G. Zhang), wuliang@genomics.cn (L. Wu).

[1] These authors contributed equally to this work.

https://doi.org/10.1016/j.cellin.2022.100005
Received 22 November 2021; Received in revised form 27 December 2021; Accepted 18 January 2022
Available online 21 January 2022

atlas of immune PBMC subclusters in HIV-1-TB co-infection and demonstrate that monocyte subsets in peripheral blood might serve as a discriminating biomarker for diagnosis of HIV-1-TB co-infection.

1. Introduction

Human immunodeficiency virus type 1 (HIV-1), the causative agent of acquired immunodeficiency syndrome (AIDS), was discovered in the 20th century (Korber et al., 2000). *Mycobacterium tuberculosis* (Mtb), the obligate pathogen of tuberculosis (TB), has co-evolved with its host for millennia (Russell, 2007). AIDS and TB remain the major health threats globally, with a global count of 37.7 million HIV-1-positive people in 2020 and approximately 20 million deaths from AIDS (Nwimo et al., 2020). There were estimated 10 million new TB cases and 1.40 million deaths worldwide in 2019 (World Health Organization, 2020). The synergy between HIV-1 and Mtb leads to further aggravation of immunological functions and greatly enhances mortality; further, Mtb infection is the primary cause of death in people living with HIV-1. HIV-1-infected people show higher frequency (~26 times) of active TB cases than those without HIV-1 infection (Lawn et al., 2011). Approximately 0.21 million deaths resulted from HIV-1 co-infection with Mtb in 2020 (World Health Organization, 2020).

Both these pathogens can manipulate host immune responses via mechanisms that are not sufficiently understood. HIV-1 induces dysfunction of the host immune system, particularly destroying $CD4^+$ T cells. Moreover, macrophages and monocytes are also targeted by HIV-1, maintaining an HIV-1 reservoir and contributing to HIV-1 persistence. An increasing number of reports have indicated that HIV-1 infection is a chronic inflammatory disease leading to immunodeficiency (Bell & Noursadeghi, 2018). Inflammatory identifiers increase during the asymptomatic stage of infection (Douek et al., 2009), and they are related to progressive HIV-1 infection (Deeks et al., 2004). The primary mechanism considers that microbial products translocate through the damaged gastrointestinal tract, and incomplete HIV-1 reverse transcripts are recognized by IFI16, which further activate inflammasome, causing pyroptosis and IL-1β secretion (Doitsh et al., 2014; Monroe et al., 2014). This leads to CD4 T cell death and activation of chronic inflammation (Bell & Noursadeghi, 2018; Doitsh & Greene, 2016; Galloway et al., 2015). Moreover, T cell death can result from HIV-1 proviral DNA integration-mediated apoptosis (Cooper et al., 2013). Chronic immune activation may cause premature immune senescence or compensatory immunoregulation (Beyer et al., 2016; Deeks, 2011; Khaitan & Unutmaz, 2011).

Mtb pathogenesis involves modulating and escaping host immune responses to facilitate the spread of bacteria by expressing diverse virulent factors (Esmail et al., 2018). Alveolar macrophages are the first innate immune cells encountered by Mtb after its inhalation. After phagocytosis by macrophages, Mtb is either cleared or proliferates within the macrophage. If macrophages fail to clear the bacteria, a mass of inactivated macrophages and neutrophils is accumulated at the infection site (O'Garra et al., 2013) and immature resident dendritic cells and other antigen-presenting cells convey bacteria via the lymphangion to local lymph nodes, which contribute to bacterial replication and transmission (Smith et al., 1970). Approximately four weeks after infection, Mtb-specific cell-induced immune responses can be identified within animals, including humans (Marais et al., 2004). During this stage, antigen-specific lymphocytes are quickly recruited to the site of infection while the number of neutrophils reduces. Particularly, $CD4^+$ T cells exert the primary function to control bacterial infection by stimulating macrophages via IFN-γ and other cytokines.

Given that macrophages and $CD4^+$ T cells are crucial for HIV-1 and Mtb infection, the two pathogens may interact with each other to impair host immunity in patients with HIV-1-TB co-infection. HIV-1-TB co-infection affects the clinical phenotype of TB; for instance, adenopathy, military pattern, and lower lung field disease became more common along with the reduced CD4 T cell number (Chamie et al., 2010). This poses challenges for diagnosis of TB in individuals with HIV-1-TB co--infection. Moreover, immunosuppression leads to decreased cavitation and sensitivity of any sputum-based Mtb detection in the context of HIV-1-TB co-infection (Esmail et al., 2018). Therefore, it is essential to identify potential new biomarkers for TB diagnosis in HIV-1 co-infected persons. Furthermore, HIV-1 may have a marked impact on host immune responses against Mtb during co-infection, including phagocytic ability, antigen presentation, cytokine generation, effect on lymphocytes of innate immune system, and role of B and T cells, which makes it more complicated to cure, leading to worse consequences (Esmail et al., 2018). In addition, Mtb infection can improve HIV-1 replication and accelerate AIDS progression (Collins et al., 2002; Goletti et al., 1996; Lawn et al., 2001; Marais et al., 2016; Meng et al., 2016; Nakata et al., 1997; Sullivan et al., 2015; Toossi et al., 2013). Better characterization of the immune responses in individuals with HIV-1-TB co-infection will contribute to finding novel immune-based methods to improve diagnosis and reduce pathological immunity.

Blood samples have high immune cell content. Better characterization of blood immune cells and their transcriptome in healthy individuals and those with different diseases will offer new insights in HIV-1-TB co-infection and will contribute to the identification of new TB biomarkers and improvement of immune-based therapy. In the present study, we applied scRNA-seq to PBMCs from individuals with HIV-1 alone and HIV-1-TB co-infection with or without anti-TB treatment in an unbiased, surface-marker-free method to characterize the transcriptome of different immune cell subclusters.

2. Results

2.1. Landscape of peripheral immune profiles in HIV-pre, HIV-pre & TB-pre, and HIV-pre & TB-pos groups

A total of 61,397 PBMCs from 11 individuals, including five patients with HIV-1 infection alone (HIV-pre, 27,934 cells), three patients with HIV-1-TB co-infection without anti-TB treatment (HIV-pre & TB pre, 19,723 cells), and three patients with HIV-1-TB co-infection and anti-TB treatment for two weeks (HIV-pre & TB pos, 9435 cells), were obtained and sequenced (Fig. 1A). A proportion of non-singlet and low-quality cells was removed, and finally, 57,092 cells were subjected for further analysis (Fig. S1). Publicly available scRNA-seq data of PBMCs from healthy controls (HC) were obtained and analyzed using the same method (Zhu et al., 2020). After unsupervised clustering, we identified three major different cell clusters for all groups (Fig. 1A, Fig. S2A). T cells expressed *CD3D* and CD3G (Fig. 1B, C, Fig. S2B); myeloid cells expressed CD68, LYZ, S100A9, FCGR3A, and S100A8 (Fig. 1B and C, Fig. S2B); and B cells expressed *CD79A, MS4A1,* and *CD79B* (Fig. 1B and C, Fig. S2B).

Additionally, many cell-type-specific marker genes were identified (Fig. 1C), including myeloid cell markers (*FCN1*, *AIF1*, and *LST1*), B cell markers (*BANK1, RALGPS2, TCF4*, and *IRF8*), and T cell markers (*IL-17R*). These additional markers might be used as PBMC-specific markers in future studies.

T cells were the major part of PBMCs from HC, followed by myeloid and B cells (Figs. 1A and S2A), consistent with previous studies (Cai et al., 2020). In contrast, we also found a lower proportion of CD4 naïve T cells within HIV-1 and HIV-1-TB co-infections (Fig. 1D), which is consistent with the case that the number of CD4 T cells decline in HIV-1 infection. A small proportion of B cells was found in HIV-pre & TB-pos group, followed by HIV-pre and HIV-pre & TB-pre groups as compared to that in HC (Fig. 1D). Moreover, B cells significantly decreased in HIV-pre & TB-pos group than in HIV-pre group (Fig. 1D). However, a higher level of

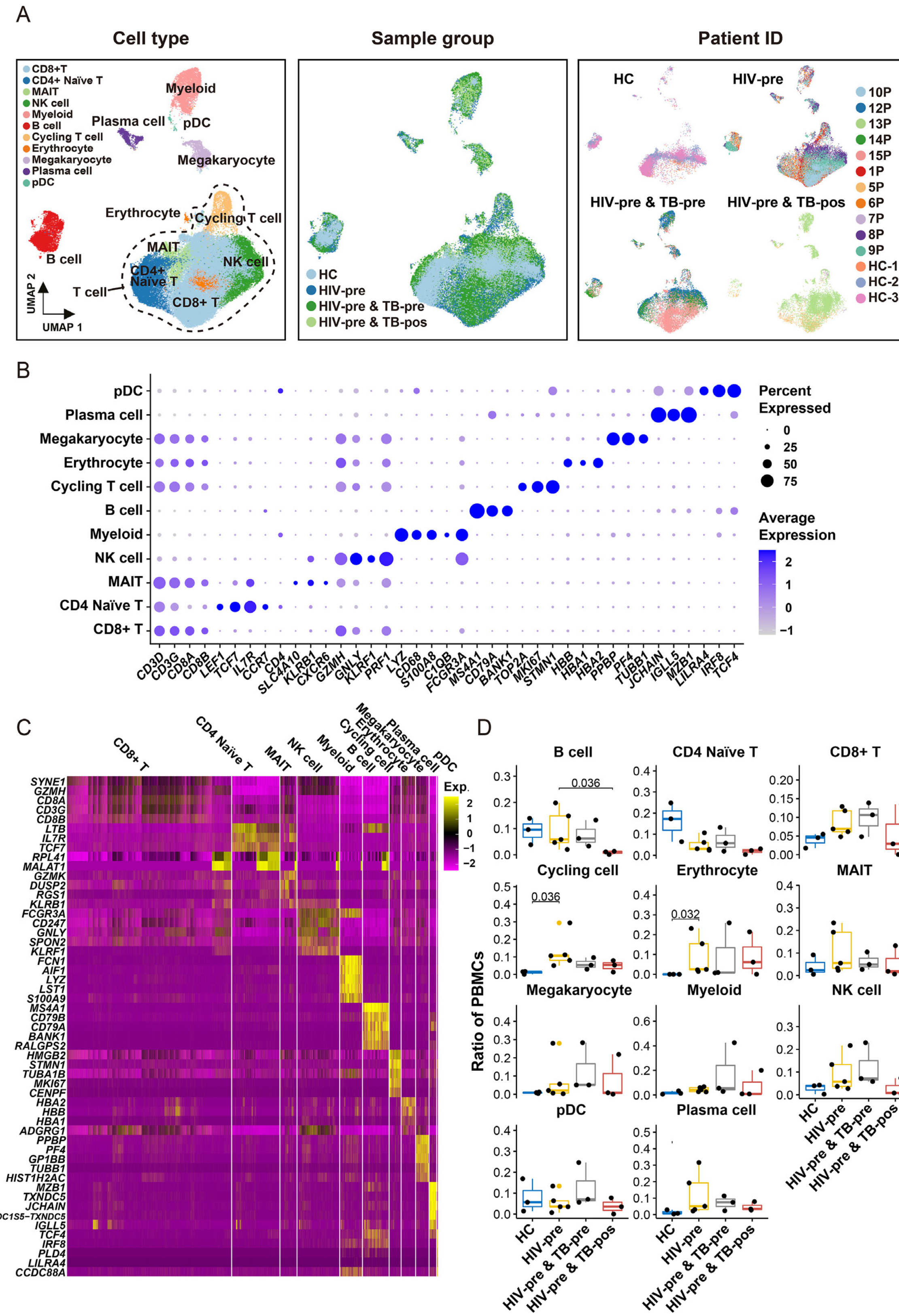

Fig. 1. Landscape of peripheral immune profiles in HIV-pre, HIV-pre & TB-pre, and HIV-pre & TB-pos groups. (A) Uniform manifold approximation and projection (UMAP) embedding of 67,810 single cells from 14 individuals (HC, n = 3; HIV-pre, n = 5; HIV-pre & TB-pre, n = 3; HIV-pre & TB-pos, n = 3). Cell types, cells from different sample groups, and individuals are indicated by color. (B) Bubble plot showing the percentage (size) and relative expression levels (color) of marker genes in each cell type. (C) Differential gene expression analysis was used to assay contrasting cells from HIV-pre, HIV-pre & TB-pre, and HIV-pre & TB-pos groups for different cell types. Heatmaps demonstrate differentially regulated genes in different cell types. (D) Boxplot showing the abundance of each cell type in peripheral blood mononuclear cells (PBMCs) from four sample groups (Wilcoxon test).

CD8$^+$ T cells was observed in HIV-pre and HIV-pre & TB-pre groups as compared to that in HIV-pre & TB-pos group and HC (Fig. 1D). Higher frequencies of cycling cells, erythrocytes, and plasma cells were also detected in HIV-pre and HIV-1-TB co-infection than in HC (Fig. 1D). Moreover, the frequencies of cycling and erythrocyte cells significantly increased in HIV-pre group than in HC group (Fig. 1D). The atlas of scRNA-seq data of PBMCs from HIV-pre group was similar to that reported in a previous study (Wang et al., 2020); however, the atlas of

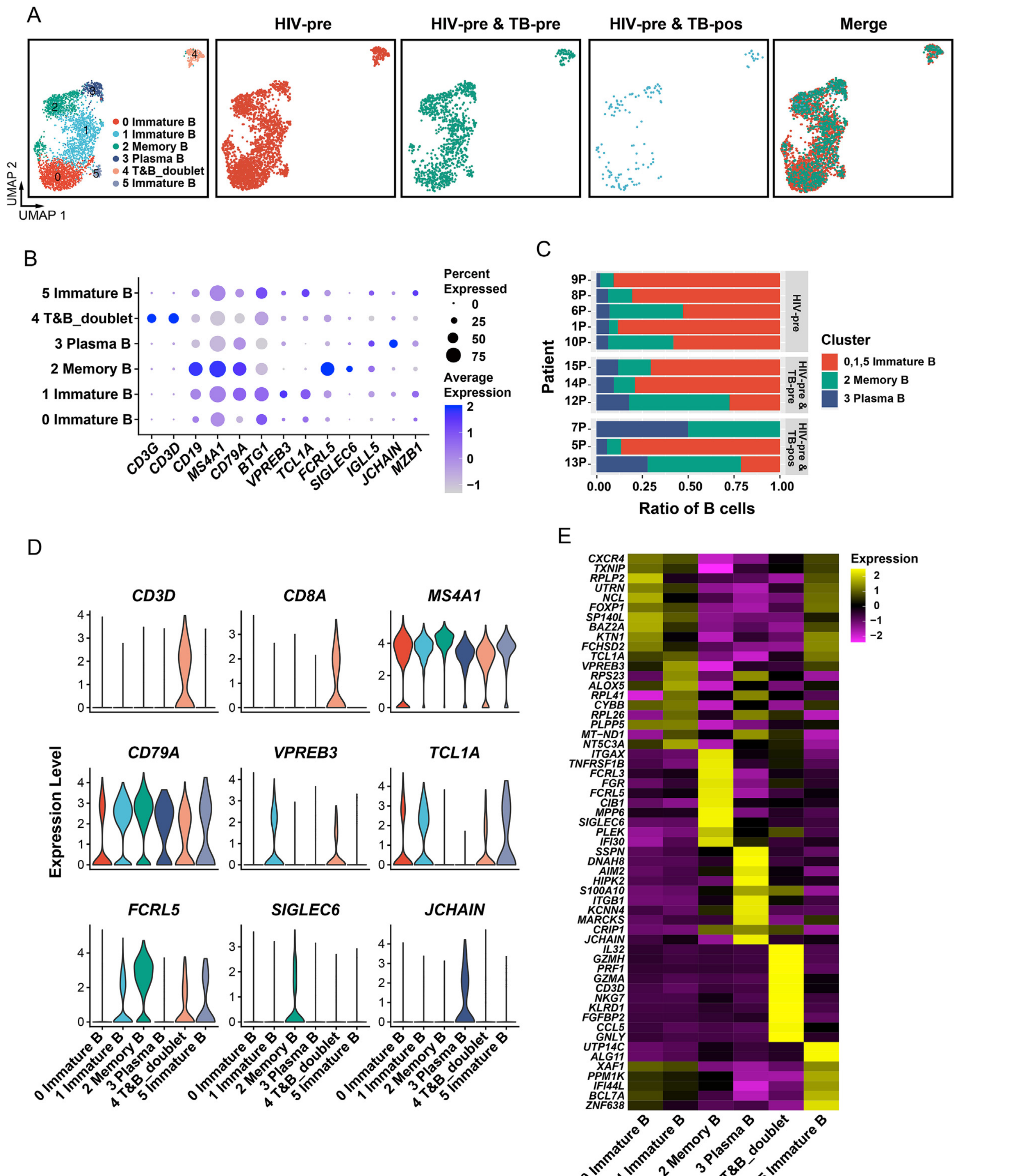

Fig. 2. Plasma B cells are gradually increased from the HIV-pre to HIV-pre & TB-pos group. (A) UMAP plot showing subclusters of B cells in different groups. Cell clusters and cells from different groups are indicated by color. (B) Bubble plot showing the percentage (size) and relative expression levels (color) of marker genes in each subcluster of B cells. (C) Proportion of cells for B cell subsets in HIV-pre, HIV-pre & TB-pre, and HIV-pre & TB-pos groups. (D) Violin plot showing the relative expression level of marker genes in each subcluster of B cells. (E) Differential gene expression analysis was performed on contrasting B cell subclusters from different groups. Heatmaps of differentially regulated genes in B cell subclusters are presented.

PBMCs from HIV-1-TB co-infection is reported for the first time in the present study. Together, these results suggest the dysregulation of HIV-1- and HIV-1-TB-associated circulating cell subclusters in HIV-1 and HIV-1-TB disease progression.

2.2. Number of plasma B cells are gradually increased from HIV-pre to HIV-pre & TB-pos groups

Since it is difficult to manage B cells, only a small proportion of studies have investigated the functions of B cells in TB; thus, their effect against Mtb infection remains unclear (du Plessis et al., 2016; Cai et al., 2020). The proportion of B cell subsets change, and consistent B cell dysfunction is observed during HIV-1 infection (Townsley et al., 2021; Sharan et al., 2020). In this study, we identified six different B cell subsets displaying various states of B cell functions (Fig. 2A, Fig. S3A). Plasma B cells (subset 3) expressed high levels of *CD79A, MS4A1, KCNN4,* and *JCHAIN* and low levels of *TCL1A* and *VPREB3* (Fig. 2B, 2D, 2E), suggestive of effective B cells (Teitell, 2005; Liu et al., 2021). Immature B cells (subset 0, 1, 5) expressed high levels of *TCL1A* and *BTG1* and low levels of *JCHAIN* and *SIGLEC6* (Fig. 2B, D, 2E), indicating that these may be early B cells (pre-B cells and naïve B cells) (Hystad et al., 2007; Chong & Sciammas, 2011). Memory B cells (subset 2) expressed high levels of *CD19, CD79A, MS4A1, FGR, FCRL3, FCRL5,* and *SIGLEC6* and low levels of *TCL1A* (Culton et al., 2007; Kim et al., 2019) (Fig. 2B, 2D, 2E), suggesting that these may be dysfunctional atypical memory B cells (Portugal et al., 2017). Subset 4 expressed high levels of B cell markers (*CD79A* and *MS4A1*) and T cell markers (*CD3D, CD8A,* and *GZMH* etc.), indicative of a T & B doublet, possibly due to a technical limitation.

According to scRNA-seq data, all six B cell subclusters existed within all three groups, and they had variable cell subset proportions (Fig. 2C, Fig. S3A). The number of immature B cell subsets (0, 1, and 5) gradually decreased from HIV-pre group to HIV-pre & TB-pre and HIV-pre & TB-pos groups (Fig. S3B), although it was not significant. A opposite trend was observed in plasma B cell subset among the three groups (Fig. S3B). Moreover, the frequency of plasma B cell subset significantly decreased in HIV-pre group as compared to that in HIV-pre & TB-pre group (Fig. S3B). Taken together, our scRNA-seq data confirmed six B cell subclusters expressing different markers in PBMCs and a increase in the number of plasma B cell subset in HIV-pre & TB-pre group, which may facilitate investigation of the functions of B cell subsets in HIV-1-TB co-infection.

2.3. Ten T/NK cell subclusters confirmed via PBMC scRNA-seq

T cells play a crucial part in restricting Mtb infection in TB patients (Cai et al., 2020), and HIV-1 infection leads to a progressive decrease in absolute $CD4^+$ T cell numbers (Sonnenberg et al., 2005). Moreover, during HIV-1-TB co-infection, $CD4^+$ T cells contribute to HIV-1 proliferation and Mtb-specific $CD4^+$ T cells are depleted, whereas the function of $CD8^+$ T cells has rarely been studied (Esmail et al., 2018). In this study, scRNA-seq data revealed that T cells could be sub-divided into 10 subsets based on the distinct expression of associated markers (Fig. 3A, Fig. S4A). Nine of these subsets expressed high levels of *CD3D* and *CD3G* (Fig. 3B, 3D, 3E). We then identified eight different $CD8^+$ T cell subsets (0–2 and 5–9). Subset 0 (CD8 T cell) expressed high levels of *CD8A* and *NKG7* (Fig. 3B, 3D, 3E, Figs. S4B and S4C). Subset 1 (active CD8 T cells) produced high levels of *CD8A, CD8B, PRF1*, and *TIGIT* (Zheng et al., 2020; Inoue et al., 2016), suggesting that these may be activated CD8 T cells (Fig. 3B, 3D, 3E, Figs. S4B and S4C). Subset 2 (cytotoxic CD8 T cells) expressed high levels of *CD8A, CD8B, GZMA, GZMB*, and *FCGR3A*, indicative of cytotoxic activity in response to pathogen infection (Ikeda et al., 2017; Thomas & Massagué, 2005; Weng et al., 2012; Pizzolato et al., 2019) (Fig. 3B, 3D, 3E, Figs. S4B and S4C). Subset 4 (Naïve T cells) expressed high levels of *CCR7, LEF1*, and *SELL*, which are known to exert a critical effect on the early stages of T cell development and homing of naïve T cells to peripheral lymphoid organs (Singh et al., 2020; Ramirez et al., 2014) (Fig. 3B, 3D, 3E, Figs. S4B and S4C). Subset 8 (exhausted CD8 T cells) expressed high levels of *CD8A, HAVCR2, CTLA4, LAG3*, and *TIGIT*, suggesting functional dysfunction of pathogen-specific CD8 T cells in chronic infection (Naing et al., 2018; Kong et al., 2016; Zhang et al., 2019; Khan et al., 2017; Blackburn et al., 2009) (Fig. 3B, D, 3E, Figs. S4B and S4C). Subset 9 (IFN + CD8 T cells) expressed high levels of *CD8A, GZMA, PRF1,* and *NKG7*. Moreover, this subset also highly expressed IFN-inducible genes, including *ISG15, MX1, IFIT3, IFIT1*, and *RSAD2*, suggesting the activation of the IFN signaling pathway (Pinto et al., 2011) (Fig. 3B, 3D, 3E, Figs. S4B and S4C). Subsets 6 and 7 expressed high levels of *CD8A, PPBP*, and *HBB*, revealing megakaryocyte-like and erythrocyte-like T cells, respectively. MAIT cell (Subset 5) expressed high levels of *SLC4A10*. Additionally, a proportion of NK cells (Subset 3) expressing high levels of *KLRF1* (Kirkham & Carlyle, 2014; Vitale et al., 2001), which plays a critical part in the control of pathogen infection, was identified (Fig. 3B, 3D, 3E, Figs. S4B and S4C). Ten T/NK cell subsets were present in all the three groups, albeit at varying proportions (Fig. 3C). Our data showed that cytotoxic and active CD8 T cell numbers decreased in HIV-pre group compared to those in the HIV-pre & TB-pre group, while IFN CD8 T cell numbers were augmented in the HIV-pre group compared to that in the HIV-pre & TB-pre group (Fig. S4D). Although the differences did not reach statistical significance among the three groups due to the limited sample size, these data will serve as a reference to investigate the role of T/NK cell subsets in HIV-1-TB co-infection in future studies.

2.4. Seven subclusters of naïve T cells identified using PBMC scRNA-seq

Early activation of naïve T cells involves better control of Mtb growth (Urdahl et al., 2011), while lymphoid tissue injury caused due to HIV-1 infection depletes the number of naïve T cells (Zeng et al., 2012). In this study, naïve T cells were further divided into seven subsets, and all of them were present in the three groups (Fig. 4A, Fig. S5A). Subset 0 (Naïve $CD4^+$ T cell) expressed high levels of *CD3D, CD4*, and *SELL* (Elyahu et al., 2019) (Fig. 4B, 4D, 4E, Figs. S5B and S5C). Subset 2 (Naïve $CD8^+$ T cell) expressed high levels of *CD8A, LEF1*, and *SELL* (Fig. 4B, 4D, 4E, Figs. S5B and S5C). Subset 3 (Cytotoxic CD8 T cells) expressed high levels of *CD8A, GZMA*, and *NKG7* (Deng et al., 2021) (Fig. 4B, 4D, 4E, Figs. S5B and S5C). Subset 4 (regulatory T cells) produced high levels of *CD3D, FOXP3, IL2RA, CTLA4, RTKN2, IKZF2*, and *TIGIT*, suggesting that these cells may repress protective responses that contribute to pathogen replication and dissemination (Schumann et al., 2020; Shelyakin et al., 2021) (Fig. 4B, 4D, 4E, Figs. S5B and S5C). Subset 6 (IFN high T cells) expressed high levels of *CD3D, IFIT3, ISG15, RSAD2, MX1*, and *IFIT1* (Fig. 4B, 4D, 4E, Figs. S5B and S5C). Subset 1 (Undefined T cells) expressed high levels of CD3D. Subset 5 (Megakaryocyte) expressed high levels of *CD3D* and *PPBP*, suggesting that these may be megakaryocyte-like cells. We also found that the number of naïve CD4 T cells increased but that of regulatory T cells decreased in the HIV-pre & TB-pre group compared to that in the HIV-pre group without statistical significance (Fig. S5D). Further investigations are required to elucidate the function of naïve CD4 and regulatory T cells in HIV-1-TB co-infection.

2.5. Nine subclusters of myeloid-derived cells identified via PBMC scRNA-seq

A large number of myeloid cells highly express the inflammatory biomarkers S100A8, S100A9, and S100A12 (Maertzdorf et al., 2016; Kaforou et al., 2013; Cai et al., 2020) in Mtb infection. Myeloid cells are also associated with inhibiting an early step of HIV-1 life cycle (Laguette et al., 2011). Moreover, increased cell death of macrophages and monocyte turnover have been observed in HIV-1-TB co-infection (Khan & Divangahi, 2018). To further characterize the remodeling of the myeloid cell cluster, we sub-clustered the myeloid cell cluster and investigated the changes in the frequencies of subsets among HIV-pre vs HIV-pre & TB-pre vs HIV-pre & TB-pos groups (Fig. 5A, Fig. S6A). We detected two monocyte subsets, characterized as non-classical (CD14low FCGR3A

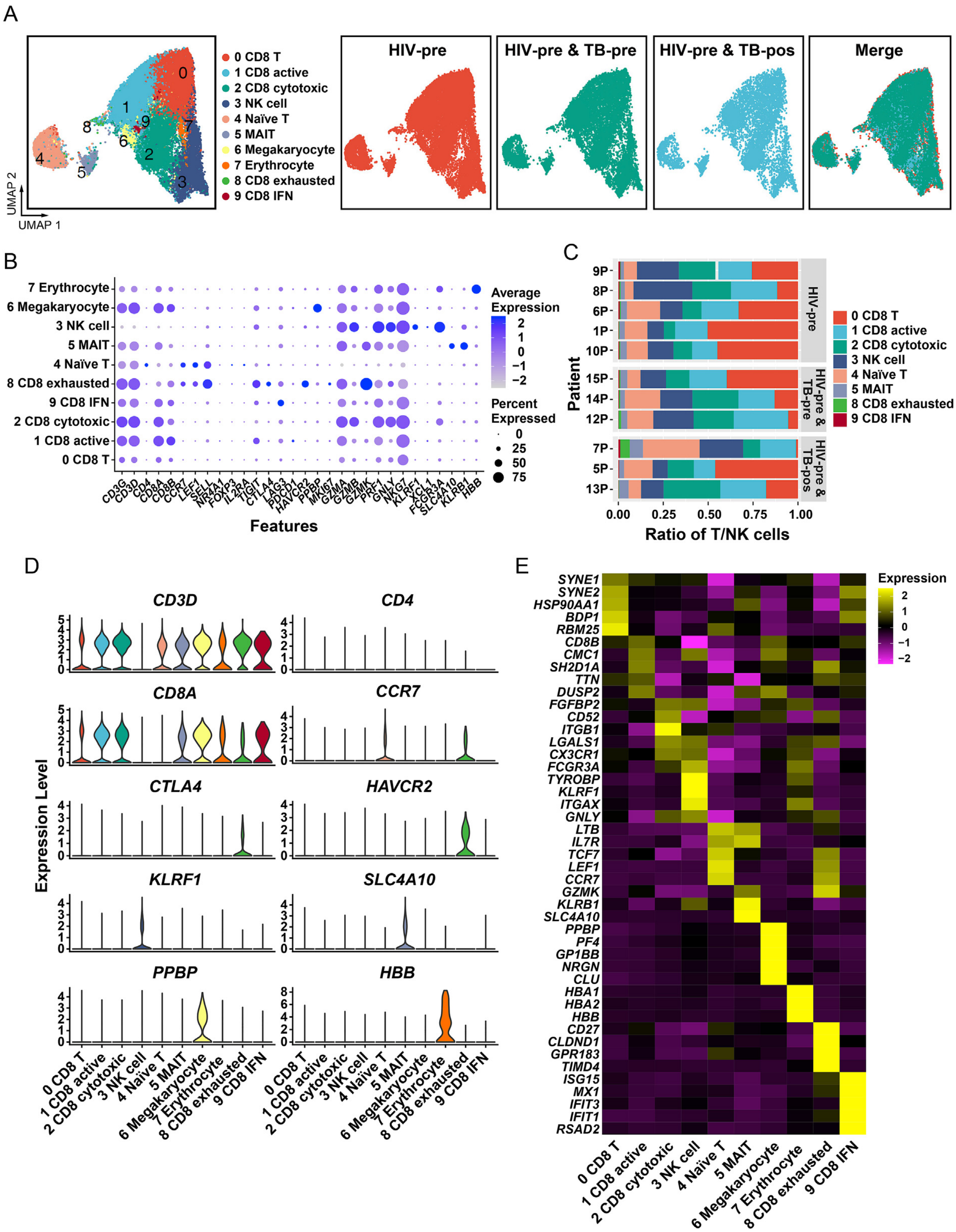

Fig. 3. Ten T/NK cell subclusters confirmed via PBMC scRNA-seq. (A) UMAP plot showing the subclusters of T/NK cells in different groups. Cell clusters and cells from different groups are indicated by color. (B) Bubble plot showing the percentage (size) and relative expression levels (color) of marker genes in each subcluster of T/NK cells. (C) Proportion of cells of the T/NK cell subsets in HIV-pre, HIV-pre & TB-pre, and HIV-pre & TB-pos groups. (D) Violin plot showing the relative expression levels of marker genes in each subcluster of T/NK cells. (E) Differential gene expression analysis of contrasting T/NK cell subclusters in different groups. Heatmaps of differentially regulated genes in T/NK cell subclusters are presented.

(CD16)+) and intermediate ($CD14^{+}CD16^{+}$) monocytes, and the classical ($CD14^{+}CD16^{-}$) monocytes were not obviously observed among the three groups (Fig. 5B and C, Figs. S6C–E). The classical monocyte subset might be included in the intermediate monocyte subset. scRNA-seq analysis showed that non-classical CD14lowCD16+ cells could re-cluster into five subsets (0–4) according to different levels of marker expression (Fig. 5B

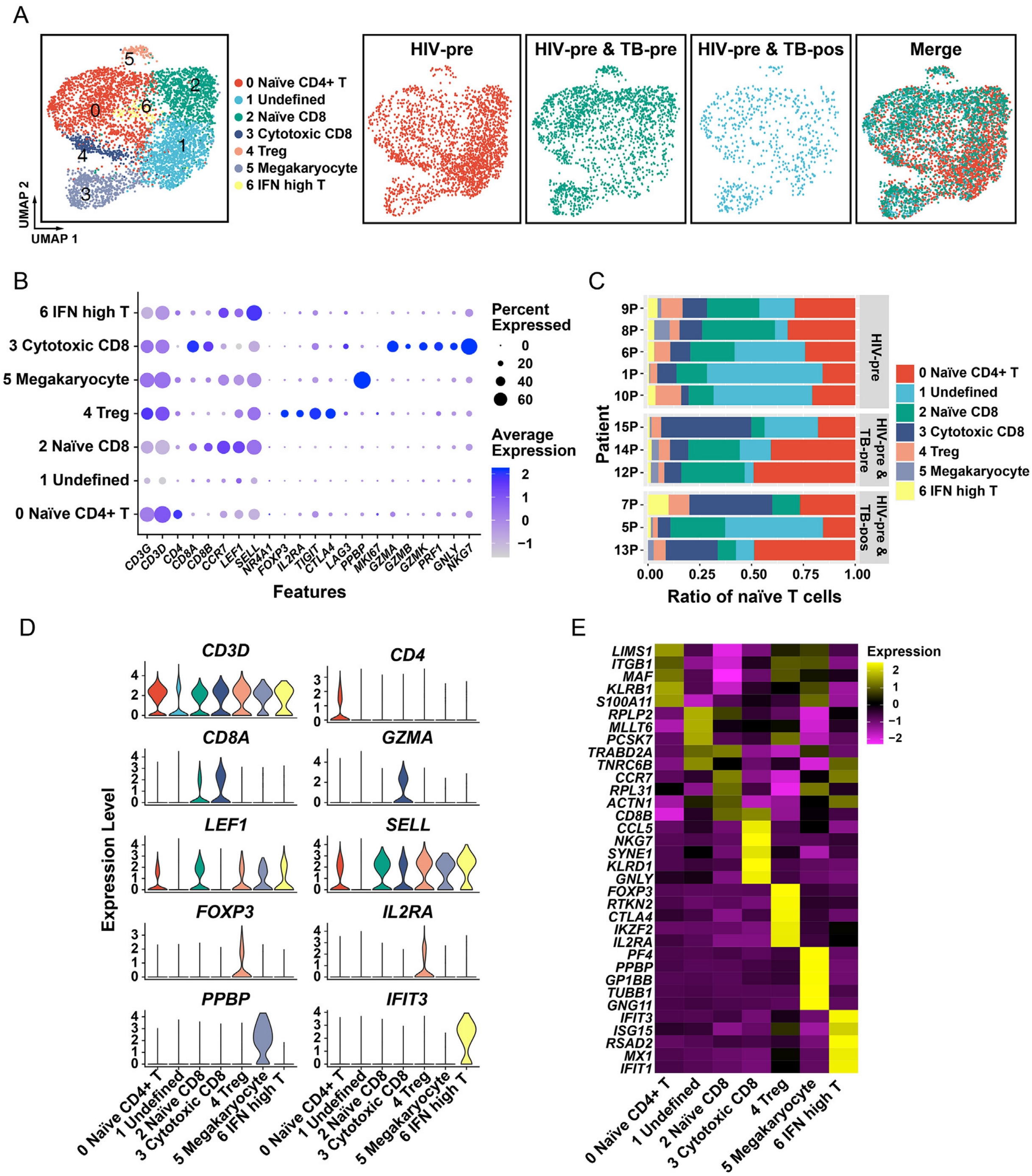

Fig. 4. Seven subclusters of naïve T cells identified via PBMC scRNA-seq. (A) UMAP plot showing subclusters of naïve T cells in different groups. Cell clusters and cells from different sample groups are indicated with color. (B) Bubble plot showing the percentage (size) and relative expression levels (color) of marker genes in each subcluster of naïve T cells. (C) Proportion of naïve T cell subsets in HIV-pre, HIV-pre & TB-pre, and HIV-pre & TB-pos groups. (D) Violin plot showing the relative expression levels of marker genes in each subcluster of naïve T cells. (E) Differential gene expression analysis of contrasting naïve T cell subsets in different groups. Heatmaps of differentially regulated genes in naïve T cell subclusters are presented.

and C, Figs. S6C–E). Particularly, subsets 0 and 2–4 expressed high levels of *LYZ*, S100A8 and S100A9, suggesting that these may be inflammatory monocytes (Cai et al., 2020) (Fig. 5B and C, Figs. S6C–E). Subset 1 contained inflammatory monocytes/macrophages highly expressing *CTSD, JUND*, and *CD68* markers (Cai et al., 2020) (Fig. 5B and C, Figs. S6C–E). Intermediate monocytes (5) expressed high levels of *PF4, CD14*, and *FCGR3A* markers (Fig. 5B and C, Figs. S6C–E). Moreover, this subset also expressed high levels of inflammatory markers, including S100A8, S100A9, S100A12, and LYZ, which are associated with disease progression. Based on specific marker expression, we also found a DC subset (6) (*CD1C* and *CLEC10A*) (Piccioli et al., 2007; Villani et al., 2017), a pDC subset (7) (*JCHAIN, LILRA4*, and *CLEC4C*) (Chappell et al., 2014; Källberg & Leanderson, 2008; Reizis, 2010) and a stem cell-like subset (8) (*CD34;* among myeloid cells) (Brown et al., 1991). Taken together, scRNA-seq analysis identified nine subsets in myeloid cells expressing different markers.

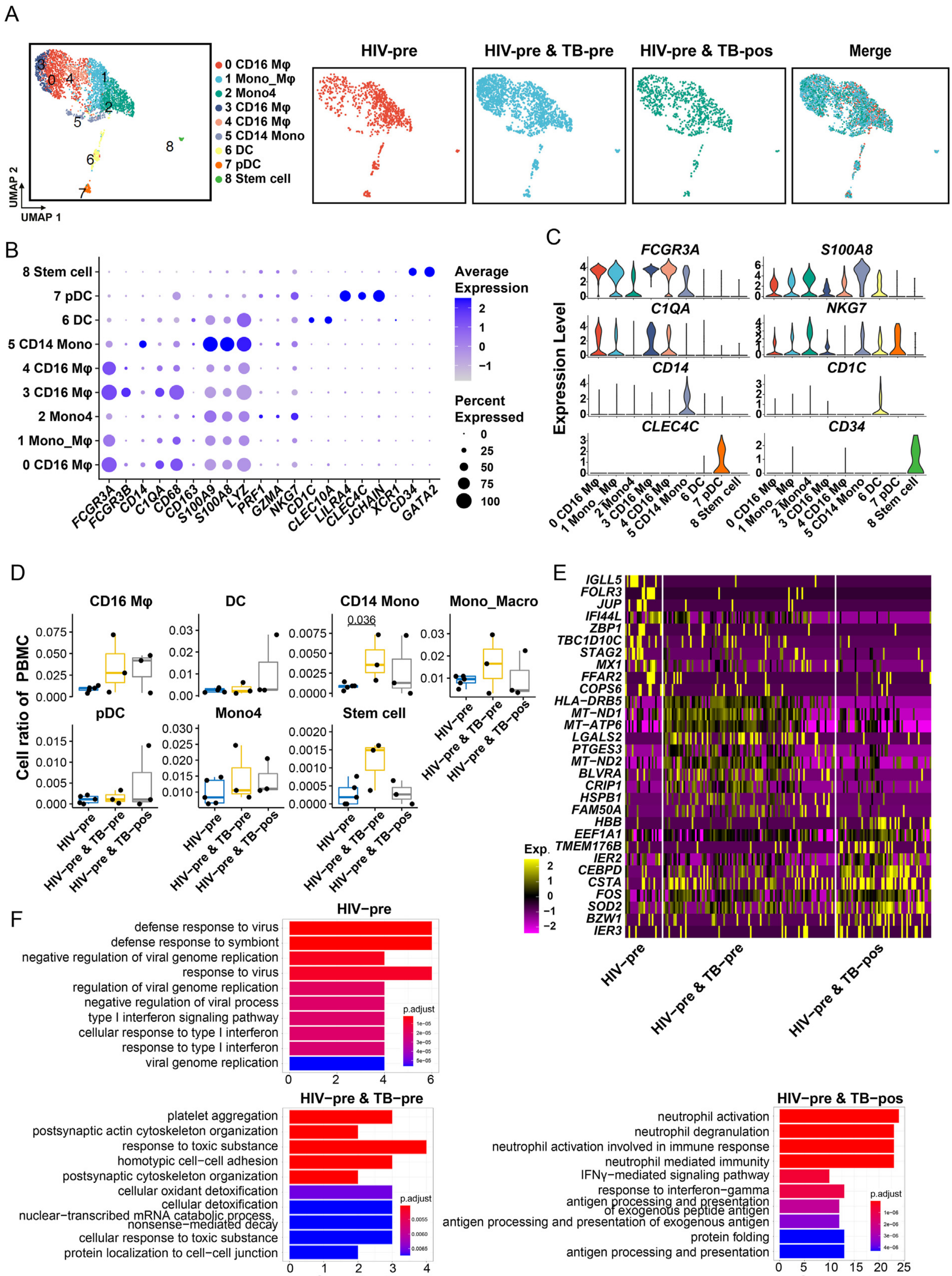

Fig. 5. Nine subclusters of myeloid-derived cells identified via PBMC scRNA-seq. (A) UMAP plot showing subclusters of myeloid cells in different groups. Cell clusters and cells from different sample groups are indicated with color. (B) Bubble plot showing the percentage (size) and relative expression levels (color) of marker genes in each subcluster of myeloid cells. (C) Violin plot showing the relative expression levels of marker genes in each subcluster of myeloid cells. (D) Boxplot showing the abundance of each cell type among PBMCs from four sample groups (Wilcoxon test). (E) Differential gene expression analysis of the contrasting CD14 Mono subset in different groups. Heatmaps of up- and down-regulated genes among the three groups are presented. (F) Bar plot showing the top ten GO biological process enrichment terms for differentially expressed genes of CD14 Mono cluster among the three groups.

2.6. Increased CD14 Mono and decreased Mono_MΦ of myeloid cells observed in HIV-pre & TB-pre group

We found that the frequency of CD14 Mono cell subset in whole PBMCs from the HIV-pre & TB-pre group was augmented compared to that in the HIV-pre group (Fig. 5D). Although the proportion of the CD14 Mono cell subset in myeloid cells increased, the difference between the two groups was no significant (Figs. S6B and S7A). Interestingly, we found that the proportion of Mono_MΦ in myeloid cells significantly decreased in patients with HIV-TB co-infection (HIV-pre & TB-pre group) compared to that in the HIV-pre group (Fig. S7A). Additionally, we found that the proportion of a DC subset decreased in patients with HIV-1-TB co-infection (HIV-pre & TB-pre) compared to that in the HIV-pre group, although the difference was not significant (Fig. S7A). Biological process (BP) enrichment analysis revealed that Mono_CD14 cells were mainly enriched in response to virus, viral replication, and type I interferon signaling, suggesting their involvement in the activation of HIV-1-contained CD14 Mono ($CD14^+$, $CD16^+$) cells and chronic immune activation (Imp et al., 2017) (Fig. 5E and F). Further, cells in the HIV-pre & TB-pre group were mostly enriched in neutrophil activation and degranulation, antigen processing and presentation, and interferon-gamma-mediated signaling, indicating their involvement in bacterial infection and subsequent monocyte recruitment, activation, and inflammation (Henderson et al., 2003) (Fig. 5E and F). Similarly, BP enrichment analysis demonstrated that Mono_MΦ was mainly enriched in type I interferon signaling pathway and response to virus in the HIV-pre group, while it was mainly enriched in antigen processing and presentation and intrinsic apoptotic signaling pathway in the HIV-pre & TB-pre group. This result indicated that Mono_MΦ cells were activated in response to HIV-1 and HIV-1-TB co-infection, and apoptosis likely contributes to the decreased Mono_MΦ numbers in the HIV-pre & TB-pre group (Figs. S7B and S7C). Altogether, our data show that the numbers of CD14 Mono and Mono_MΦ particularly increased and decreased, respectively, in the HIV-pre & TB-pre group, and this finding warrants further investigation.

2.7. Monocyte subset proportions sufficiently distinguish HIV-1 from HIV-1-TB co-infection

We validated the role of monocyte cell subset in HIV-1/HIV-1-TB co-infection using another cohort. Consistent with our original sc-RNAseq results, our validation results demonstrated that the frequency of monocytes significantly increased in the HIV-pre & TB-pre group as compared to that in HIV-pre group (Fig. 6A). To further estimate the diagnostic efficacy of the monocyte subcluster in discriminating HIV-1-TB co-infection from HIV-1 infection, receiver-operating characteristic (ROC) curve analysis was performed for this cohort. The ROC curve analysis of the HIV-pre vs HIV-pre & TB-pre group suggested that monocytes could act as a potential molecular marker (area under the curve, 0.8046; Fig. 6B). Therefore, the monocyte cell subset is an effective marker for distinguishing HIV-1-TB co-infection from HIV-1 infection.

3. Discussion

In the present study, to characterize the effect of HIV-1-TB co-infection on circulating immune-cell profiles, we subjected $> 60{,}000$ PBMCs obtained from donors in HIV-pre, HIV-pre & TB-pre, and HIV-pre & TB-pos groups to scRNA-seq analysis and determined their transcriptomic characteristics and the ratio of PBMC subclusters among the three groups. The scRNA-seq analysis identified three primary cell types—T cells, B cells, and myeloid cells—and they were further sub-divided into 32 subclusters according to specific gene expression. Moreover, our scRNA-seq data confirmed many additional markers, including myeloid cell markers (*FCN1, AIF1*, and *LST1*), B cell markers (*BANK1, RALGPS2, TCF4*, and *IRF8*), and T cell markers (*IL-17R*). These markers may be used for further studies to differentiate distinct immune cell subsets of PBMCs and explore their role in the diagnosis and protective immunity against HIV-1-TB co-infection.

The frequency of circulating cell subsets alters upon HIV-1 or Mtb infection, which causes dysregulation of the host immune system (Cai et al., 2020; Wang et al., 2020). Wang's study showed that the proportion and role of $CD4^+$, $CD8^+$ T, and B cell subclusters are significantly altered in HIV-1 infection (Wang et al., 2020). Cai et al. found that a natural killer cell subset was depleted, while the numbers of inflammatory monocytes and a B cell subset were increased in TB (Cai et al., 2020). Consistent with previous studies, our scRNA-seq data demonstrated that fluctuations in subsets of these cell types among HIV-pre, HIV-pre & TB-pre, and HIV-pre & TB-pos groups, such as increased CD14 Mono and decreased Mono_MΦ subset proportion in the HIV-pre & TB-pre group compared with that in the HIV-pre group, were closely associated with different disease states, particularly those that are likely specific for diseases. Our PBMC atlas offers new perspectives into cell subsets involved in HIV-1-TB co-infection.

The $CD14^+CD16^+$ monocyte subcluster accounts for approximately 10% of the total monocyte population in normal subjects, and these proportions are altered during HIV-1 or Mtb infection. HIV-1 can infect and replicate in $CD14^+CD16^+$ monocytes (Zhu et al., 2002). Moreover,

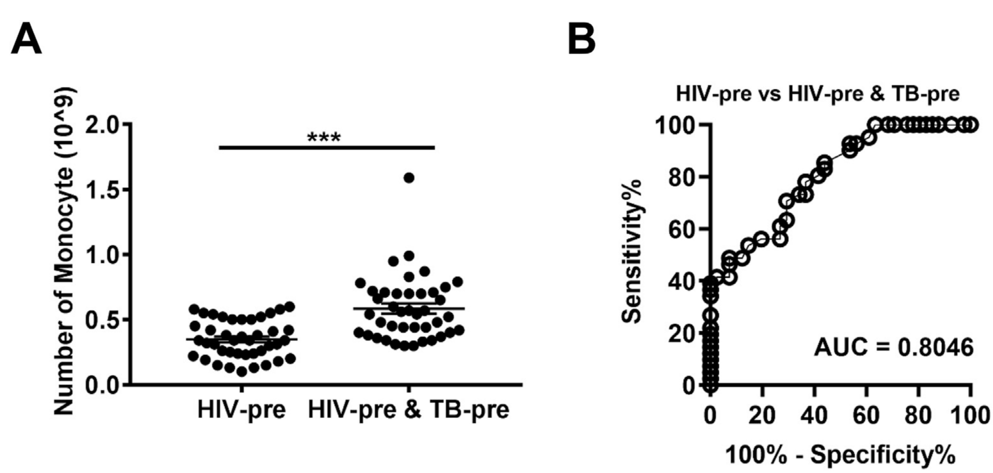

Fig. 6. Monocyte subset proportions sufficiently distinguish HIV-1 from HIV-1-TB co-infection. (A) Blood routine analysis of the counts of monocytes from HIV-pre and HIV-pre & TB-pre groups in the second cohort. Unpaired *t*-test was performed, and the data is represented as mean ± SEM. ***$P < 0.001$. (B) ROC curve of monocyte subsets to distinguish the HIV-pre & TB-pre group from the HIV-pre group (AUC = 0.8046). AUC, area under curve.

these monocytes are critical to HIV-1 pathogenesis and comorbidities (León-Rivera et al., 2020) and involved in disease progression in long-term HIV-1 infection (Han et al., 2009). The monocytes are augmented in numbers in peripheral blood during HIV-1 infection and preferentially infected with HIV-1, which may serve as a viral reservoir (León-Rivera et al., 2020). Castano et al. found that the frequency of intermediate and non-classical monocytes increased while that of classical monocytes decreased in TB patients, and intermediate monocytes may play a role in T cell activation, proliferation, and antigen presentation (Sampath et al., 2018). Similarly, another report mentioned that an increased proportion of $CD14^{+}CD16^{+}$ monocytes, which is involved in disease severity, in the total monocyte population has been observed in TB patients (Balboa et al., 2011). This subset barely stimulates a respiratory burst, shows no response to the early stages of infection, and has little potential to differentiate into functional dendritic cells (Sampath et al., 2018). Moreover, this monocyte subset tends to differentiate into M2-like macrophages, which facilitate bacterial persistence and the establishment of chronic infection (Lastrucci et al., 2015). Consistent with previous studies, our study also showed an increased frequency of $CD14^{+}CD16^{+}$ monocytes (CD14 Mono) among PBMCs of the HIV-pre group as compared to those of the HC. However, to date, very few studies have investigated the function of $CD14^{+}CD16^{+}$ monocytes in HIV-1-TB co-infection. A previous report showed that an elevated frequency of $CD14^{+}CD16^{+}$ monocytes in patients with severe HIV-1-TB is associated with mortality (Janssen et al., 2017). In this study, we first depicted the atlas of PBMCs from HIV-1-TB co-infection using scRNA-seq analysis. We also found altered proportions of circulating monocytes among the three groups. Similarly, a high proportion of $CD14^{+}CD16^{+}$ monocytes was observed in the HIV-pre & TB-pre group as compared to that in the HIV-pre group. $CD14^{+}CD16^{+}$ monocytes expressed high levels of S100A8, S100A9, S1*00A12, LYZ, PF4*, and *PPBP*, indicating that these cells have an inflammatory phenotype. Inflammatory $CD14^{+}CD16$ monocytes have also been found in patients who died from severe HIV-1-TB co-infection (Janssen et al., 2017), indicating that this subset may contribute to Mtb survival in HIV-1-TB co-infection. Interestingly, HIV-1-infected $CD14^{+}CD16^{+}$ monocytes primarily migrate across the blood-brain barrier, which is involved in the development of cognitive impairment (León-Rivera et al., 2021). In this case, TB might facilitate the development of HIV-1-associated neurocognitive disorders in patients with HIV-1-TB co-infection. Additionally, we found that Mono_MΦ highly expressed the inflammatory markers of S100A8, S100A9, and CD68 (Kaforou et al., 2013; Maertzdorf et al., 2016), the levels of which were decreased in the HIV-pre & TB-pre group as compared to that in the HIV-pre patients. This indicates that the inflammatory effect may be caused by the immediate loss of the membrane integrity of macrophages upon death, which may facilitate bacterial survival (Mahamed et al., 2017). Together, our sc-RNA-seq data revealed that the interaction between HIV-1 and Mtb in the host induced the expansion of the inflammatory $CD14^{+}CD16^{+}$ monocyte subcluster, which may contribute to both HIV-1 and Mtb pathogenesis.

Although a large number of reports are focused on the search for new TB biomarkers, the usefulness of these biomarkers remains limited. The available methods for TB examination, such as culture, smear microscopy, and nucleic acid amplification technique, are not sufficient for TB diagnosis, specifically for patients without sputum and HIV-1-TB co-infection. In this study, we found that the variation in the monocyte subset levels was distinct and specific enough to distinguish HIV-1-TB co-infection from HIV-1 infection, and it might be regarded as a useful biomarker for this purpose. Moreover, our results showed that anti-TB treatment might not affect the frequency of monocyte subsets (Fig. 5D), suggesting that the frequency of monocyte subsets is an efficient biomarker for TB diagnosis in HIV-1-TB co-infections following anti-TB therapy.

Our study has a few limitations. First, gender bias might exist, because a small number of samples were used in the study. Second, due to restrictions imposed by some objective factors, alterations in certain subsets identified in our scRNA-seq data, such as plasma B cell subset, could not be further validated. Third, our scRNA-seq data could not identify low-frequency immune-cell populations due to the limitation of resolution. More cells and high-resolution single-cell analysis tools are required to better characterize these cell subsets. Additionally, serial PBMCs were not obtained from the same patients.

In summary, to the best of our knowledge, our scRNA-seq data depicted the first atlas of PBMC immune-cell subclusters in HIV-1-TB co-infection via scRNA-seq analysis. Better characterization of circulating cell subsets may clarify the role of cell subclusters and mechanisms underlying the dysfunction of the immune response in HIV-1-TB co-infection, such as the increase in inflammatory $CD14^{+}CD16^{+}$ monocyte numbers, which might offer novel insights into TB diagnosis and immune-based therapy of HIV-1-TB co-infections.

4. Materials and methods

4.1. Subjects and specimen acquisition

The discovery cohort used for scRNA-seq analysis included patients with HIV-1 infection alone (HIV-pre, $n = 5$), HIV-1-TB co-infection without anti-TB treatment (HIV-pre & TB-pre, $n = 3$), and HIV-1-TB co-infection with anti-TB treatment for 2 weeks (HIV-pre & TB-pos, $n = 3$). The validation cohort comprised HIV-pre ($n = 40$) and HIV-pre & TB-pre ($n = 40$) for a routine blood differential test. HIV-1 diagnosis was based on positive HIV-1 RNA levels in the absence of results for positive enzyme-linked immunosorbent antibody assay and confirmatory Western-blot antibody test for HIV-1. None of the enrolled participants had received antiretroviral therapy. Diagnosis of active pulmonary TB was performed according to clinical characteristics and based on the results obtained for chest radiography, microscopy for acid-fast bacillus, nucleic acid amplification test, and Mtb culture. All confirmed pulmonary TB patients were drug-sensitive and followed a standard 6-month treatment regimen recommended by WHO (a 2-month intensive phase of isoniazid, rifampin, pyrazinamide, and ethambutol followed by a 4-month continuation phase of rifampin and isoniazid). Detailed clinical information is shown in Table S1. Peripheral blood samples were collected from the recruited individuals via venipuncture. PBMCs from the discovery cohort were isolated via density gradient centrifugation over Ficoll-Hypaque, and whole blood from the validation cohort was used for blood differential tests performed on COULTER LH 755 (Beckman Coulter, Fullerton, CA, USA).

4.2. Single-cell RNA library construction and sequencing

PBMCs were obtained from fresh blood as depicted previously (Cai et al., 2020). Cell viability (>90%) was evaluated by trypan blue staining. DNBelab C4 system was utilized for scRNA-seq library preparation as previous discribed (Liu et al., 2019, p. 818450). Briefly, the single-cell suspensions were transformed into barcoded scRNA-seq libraries via steps including droplet generation, emulsion breakage, mRNA captured beads accumulation, inverse transcription, cDNA amplification, and purification. cDNA production was sheared to short fragments with 250–400 bp, and indexed sequencing libraries were constructed in line with the manufacturer's instruction. Qualification was performed using Qubit ssDNA Assay Kit (Thermo Fisher Scientific) and Agilent 2100 Bioanalyzer. All libraries were further sequenced by the DIPSEQ T1 sequencing platform (China National GeneBank) with pair-end sequencing.

4.3. scRNA-seq data processing and cell clustering

The scRNA-seq data of PBMCs from HCs generated using the DNBelab C4 system were obtained from CNGB Nucleotide Sequence Archive (CNSA: https://db.cngb.org/cnsa) under the accession number CNP0001102 (Zhu et al., 2020). The sequenced data were processed using an open-source pipeline (https://github.com/MGI-tech-bioinformatics/DNBelab_C_Series_HT_scRNA-analysis-software). Briefly, all samples were subjected to sample de-multiplexing, barcode processing, and single-cell 3′ unique molecular identifier (UMI) counting with the default parameters. Next, the obtained reads were aligned to the GRCh38 genome reference using STAR (v2.5.3). The available cells were automatically acquired according to the UMI number distribution of each cell using the "barcodeRanks()" function of the DropletUtils tool. Finally, we used PISA to calculate the gene UMI count of cells and create a gene × cell UMI count matrix. The gene expression matrix was used for cell clustering analysis using Seurat (version 3.2.2) (Butler et al., 2018). Cells harboring less than 200 genes (UMI >0) or more than 3000 genes or over 5% UMI originated from the mitochondrial genome were identified as low quality cells. Following the removal of cells, the gene count matrix was normalized using log1p normalization, and the top 2000 highly variable genes were then selected to perform principal component analysis. We used harmony (https://github.com/immunogenomics/harmony) (Korsunsky et al., 2019) to integrate the healthy control data with our data using 30 PCs. Following this, 30 dimensions of harmony reduction were used for subsequent Louvain clustering and Uniform Manifold Approximation and Projection (UMAP) based-visualization using UMAP. The cell types were identified using known markers that were highly expressed in a specific subset. For B cell, T/NK cell, naïve T cell and myeloid cell subtypes sub-clustering, 30 PCs were firstly used for harmony reduction, and then top 20 dimensions of harmony reduction were for clustering and UMAP visualization.

4.4. Differential gene expression analysis

Differentially expressed gene (DEG) analysis in each subset/group was confirmed through the FindAllMarkers function of the Seurat package (v3.2.2) with default parameter setting.

4.5. Pathway analysis

ClusterProfiler(Yu et al., 2012) was applied to GO enrichment analysis with differentially expressed genes of a cell type among different groups. GO terms with a p value < 0.05 were significant and the top ten GO terms of biological process were shown.

4.6. Statistical analysis

The differences in the cell ratio between two groups were confirmed through Wilcoxon test. The comparison of the number of monocyte between two groups was performed through unpaired two-tailed *t*-test. Receive-operating characteristic (ROC) analysis was performed to determine the power of peripheral monocyte to distinguish HIV-1-TB co-infection from HIV-1 infection. All statistical analyses and presentations were performed using R3.6.1 or GraphPad Prism 7.

Data availability

The scRNA-seq processed expression data of HIV/TB infection patients can also obtain from CNSA with accession number CNP0002505.

Author contributions

Qinglong Guo, Yu Zhong, Zhifeng Wang, Tingzhi Cao: Methodology, Software, Validation, Formal analysis, Investigation and Writing; **Mingyuan Zhang, Peiyan Zhang, Waidong Huang, Jing Bi, Yue Yuan, Min Ou, Xuanxuan Zou, Guohui Xiao, Yuan Yang, Shiping Liu:** Methodology, Visualization, Validation; **Longqi Liu, Zhaoqin Wang, Guoliang Zhang, Liang Wu:** Conceptualization, Methodology, Writing, Supervision, Project administration and Funding acquisition.

Declaration of competing interest

None.

Acknowledgement

This work was supported by the National Natural Science Foundation of China (No. 82170009, 81873958, 81802058), the National Key Research and Development Plan (No. 2020YFA0907200), the Guangdong Scientific and Technological Foundation (No. 2019B1515120041, 2020B1111170014), the Shenzhen Scientific and Technological Foundation (No. KCXFZ202002011007083), the Sanming Project of Medicine in Shenzhen (No. SZSM201911009), and Shenzhen Key Laboratory of Single-Cell Omics (ZDSYS20190902093613831). We also thank the support provided by China National GeneBank.

Appendix A. Supplementary data

Supplementary data to this article can be found online at https://doi.org/10.1016/j.cellin.2022.100005.

References

Balboa, L., Romero, M. M., Basile, J. I., Sabio Y García, C. A., Schierloh, P., Yokobori, N., Geffner, L., Musella, R. M., Castagnino, J., Abbate, E., De La Barrera, S., Sasiain, M. C., & Alemán, M. (2011). Paradoxical role of Cd16+Ccr2+Ccr5+ monocytes in tuberculosis: Efficient Apc in pleural effusion but also mark disease severity in blood. *Journal of Leukocyte Biology, 90*, 69–75.

Bell, L. C. K., & Noursadeghi, M. (2018). Pathogenesis of Hiv-1 and Mycobacterium tuberculosis co-infection. *Nature Reviews Microbiology, 16*, 80–90.

Beyer, M., Abdullah, Z., Chemnitz, J. M., Maisel, D., Sander, J., Lehmann, C., Thabet, Y., Shinde, P. V., Schmidleithner, L., Köhne, M., Trebicka, J., Schierwagen, R., Hofmann, A., Popov, A., Lang, K. S., Oxenius, A., Buch, T., Kurts, C., Heikenwalder, M., … Schultze, J. L. (2016). Tumor-necrosis factor impairs Cd4(+) T cell-mediated immunological control in chronic viral infection. *Nature Immunology, 17*, 593–603.

Blackburn, S. D., Shin, H., Haining, W. N., Zou, T., Workman, C. J., Polley, A., Betts, M. R., Freeman, G. J., Vignali, D. A., & Wherry, E. J. (2009). Coregulation of Cd8+ T cell exhaustion by multiple inhibitory receptors during chronic viral infection. *Nature Immunology, 10*, 29–37.

Brown, J., Greaves, M. F., & Molgaard, H. V. (1991). The gene encoding the stem cell antigen, Cd34, is conserved in mouse and expressed in haemopoietic progenitor cell lines, brain, and embryonic fibroblasts. *International Immunology, 3*, 175–184.

Butler, A., Hoffman, P., Smibert, P., Papalexi, E., & Satija, R. (2018). Integrating single-cell transcriptomic data across different conditions, technologies, and species. *Nature Biotechnology, 36*, 411–420.

Cai, Y., Dai, Y., Wang, Y., Yang, Q., Guo, J., Wei, C., Chen, W., Huang, H., Zhu, J., Zhang, C., Zheng, W., Wen, Z., Liu, H., Zhang, M., Xing, S., Jin, Q., Feng, C. G., & Chen, X. (2020). Single-cell transcriptomics of blood reveals a natural killer cell subset depletion in tuberculosis. *EBioMedicine, 53*, 102686.

Chamie, G., Luetkemeyer, A., Charlebois, E., & Havlir, D. V. (2010). Tuberculosis as part of the natural history of Hiv infection in developing countries. *Clinical Infectious Diseases, 50*(Suppl 3), S245–S254.

Chappell, C. P., Giltiay, N. V., Draves, K. E., Chen, C., Hayden-Ledbetter, M. S., Shlomchik, M. J., Kaplan, D. H., & Clark, E. A. (2014). Targeting antigens through blood dendritic cell antigen 2 on plasmacytoid dendritic cells promotes immunologic tolerance. *The Journal of Immunology, 192*, 5789–5801.

Chong, A. S., & Sciammas, R. (2011). Matchmaking the B-cell signature of tolerance to regulatory B cells. *American Journal of Transplantation, 11*, 2555–2560.

Collins, K. R., Quiñones-Mateu, M. E., Wu, M., Luzze, H., Johnson, J. L., Hirsch, C., Toossi, Z., & Arts, E. J. (2002). Human immunodeficiency virus type 1 (Hiv-1) quasispecies at the sites of Mycobacterium tuberculosis infection contribute to systemic Hiv-1 heterogeneity. *Journal of Virology, 76*, 1697–1706.

Cooper, A., García, M., Petrovas, C., Yamamoto, T., Koup, R. A., & Nabel, G. J. (2013). Hiv-1 causes Cd4 cell death through Dna-dependent protein kinase during viral integration. *Nature, 498*, 376–379.

Culton, D. A., Nicholas, M. W., Bunch, D. O., Zhen, Q. L., Kepler, T. B., Dooley, M. A., Mohan, C., Nachman, P. H., & Clarke, S. H. (2007). Similar Cd19 dysregulation in two autoantibody-associated autoimmune diseases suggests a shared mechanism of B-cell tolerance loss. *Journal of Clinical Immunology, 27*, 53–68.

Deeks, S. G. (2011). Hiv infection, inflammation, immunosenescence, and aging. *Annual Review of Medicine, 62*, 141–155.

Deeks, S. G., Kitchen, C. M., Liu, L., Guo, H., Gascon, R., Narváez, A. B., Hunt, P., Martin, J. N., Kahn, J. O., Levy, J., Mcgrath, M. S., & Hecht, F. M. (2004). Immune activation set point during early Hiv infection predicts subsequent Cd4+ T-cell changes independent of viral load. *Blood, 104*, 942–947.

Deng, W., Ma, Y., Su, Z., Liu, Y., Liang, P., Huang, C., Liu, X., Shao, J., Zhang, Y., Zhang, K., Chen, J., & Li, R. (2021). Single-cell Rna-sequencing analyses identify

heterogeneity of Cd8(+) T cell subpopulations and novel therapy targets in melanoma. *Molecular Therapy—Oncolytics, 20*, 105–118.
Doitsh, G., Galloway, N. L., Geng, X., Yang, Z., Monroe, K. M., Zepeda, O., Hunt, P. W., Hatano, H., Sowinski, S., Muñoz-Arias, I., & Greene, W. C. (2014). Cell death by pyroptosis drives Cd4 T-cell depletion in Hiv-1 infection. *Nature, 505*, 509–514.
Doitsh, G., & Greene, W. C. (2016). Dissecting how Cd4 T cells are lost during Hiv infection. *Cell Host & Microbe, 19*, 280–291.
Douek, D. C., Roederer, M., & Koup, R. A. (2009). Emerging concepts in the immunopathogenesis of Aids. *Annual Review of Medicine, 60*, 471–484.
Du Plessis, W. J., Walzl, G., & Loxton, A. G. (2016). B cells as multi-functional players during Mycobacterium tuberculosis infection and disease. *Tuberculosis, 97*, 118–125.
Elyahu, Y., Hekselman, I., Eizenberg-Magar, I., Berner, O., Strominger, I., Schiller, M., Mittal, K., Nemirovsky, A., Eremenko, E., Vital, A., Simonovsky, E., Chalifa-Caspi, V., Friedman, N., Yeger-Lotem, E., & Monsonego, A. (2019). Aging promotes reorganization of the Cd4 T cell landscape toward extreme regulatory and effector phenotypes. *Science Advances, 5*, Article eaaw8330.
Esmail, H., Riou, C., Bruyn, E. D., Lai, R. P., Harley, Y. X. R., Meintjes, G., Wilkinson, K. A., & Wilkinson, R. J. (2018). The immune response to Mycobacterium tuberculosis in Hiv-1-coinfected persons. *Annual Review of Immunology, 36*, 603–638.
Galloway, N. L., Doitsh, G., Monroe, K. M., Yang, Z., Muñoz-Arias, I., Levy, D. N., & Greene, W. C. (2015). Cell-to-Cell transmission of Hiv-1 is required to trigger pyroptotic death of lymphoid-tissue-derived Cd4 T cells. *Cell Reports, 12*, 1555–1563.
Goletti, D., Weissman, D., Jackson, R. W., Graham, N. M., Vlahov, D., Klein, R. S., Munsiff, S. S., Ortona, L., Cauda, R., & Fauci, A. S. (1996). Effect of Mycobacterium tuberculosis on Hiv replication. Role of immune activation. *The Journal of Immunology, 157*, 1271–1278.
Han, J., Wang, B., Han, N., Zhao, Y., Song, C., Feng, X., Mao, Y., Zhang, F., Zhao, H., & Zeng, H. (2009). Cd14(high)Cd16(+) rather than Cd14(low)Cd16(+) monocytes correlate with disease progression in chronic Hiv-infected patients. *Journal of Acquired Immune Deficiency Syndromes, 52*, 553–559.
Henderson, R. B., Hobbs, J. A., Mathies, M., & Hogg, N. (2003). Rapid recruitment of inflammatory monocytes is independent of neutrophil migration. *Blood, 102*, 328–335.
Hystad, M. E., Myklebust, J. H., Bø, T. H., Sivertsen, E. A., Rian, E., Forfang, L., Munthe, E., Rosenwald, A., Chiorazzi, M., Jonassen, I., Staudt, L. M., & Smeland, E. B. (2007). Characterization of early stages of human B cell development by gene expression profiling. *The Journal of Immunology, 179*, 3662–3671.
Ikeda, Y., Kiyotani, K., Yew, P. Y., Sato, S., Imai, Y., Yamaguchi, R., Miyano, S., Fujiwara, K., Hasegawa, K., & Nakamura, Y. (2017). Clinical significance of T cell clonality and expression levels of immune-related genes in endometrial cancer. *Oncology Reports, 37*, 2603–2610.
Imp, B. M., Rubin, L. H., Tien, P. C., Plankey, M. W., Golub, E. T., French, A. L., & Valcour, V. G. (2017). Monocyte activation is associated with worse cognitive performance in Hiv-infected women with virologic suppression. *The Journal of Infectious Diseases, 215*, 114–121.
Inoue, H., Park, J. H., Kiyotani, K., Zewde, M., Miyashita, A., Jinnin, M., Kiniwa, Y., Okuyama, R., Tanaka, R., Fujisawa, Y., Kato, H., Morita, A., Asai, J., Katoh, N., Yokota, K., Akiyama, M., Ihn, H., Fukushima, S., & Nakamura, Y. (2016). Intratumoral expression levels of Pd-L1, Gzma, and Hla-A along with oligoclonal T cell expansion associate with response to nivolumab in metastatic melanoma. *OncoImmunology, 5*, Article e1204507.
Janssen, S., Schutz, C., Ward, A., Nemes, E., Wilkinson, K. A., Scriven, J., Huson, M. A., Aben, N., Maartens, G., Burton, R., Wilkinson, R. J., Grobusch, M. P., Van Der Poll, T., & Meintjes, G. (2017). Mortality in severe human immunodeficiency virus-tuberculosis associates with innate immune activation and dysfunction of monocytes. *Clinical Infectious Diseases, 65*, 73–82.
Kaforou, M., Wright, V. J., Oni, T., French, N., Anderson, S. T., Bangani, N., Banwell, C. M., Brent, A. J., Crampin, A. C., Dockrell, H. M., Eley, B., Heyderman, R. S., Hibberd, M. L., Kern, F., Langford, P. R., Ling, L., Mendelson, M., Ottenhoff, T. H., Zgambo, F., … Levin, M. (2013). Detection of tuberculosis in Hiv-infected and -uninfected African adults using whole blood Rna expression signatures: A case-control study. *PLoS Medicine, 10*, Article e1001538.
Källberg, E., & Leanderson, T. (2008). A subset of dendritic cells express joining chain (J-chain) protein. *Immunology, 123*, 590–599.
Khaitan, A., & Unutmaz, D. (2011). Revisiting immune exhaustion during Hiv infection. *Current HIV, 8*, 4–11.
Khan, N., & Divangahi, M. (2018). Mycobacterium tuberculosis and Hiv coinfection brings fire and fury to macrophages. *The Journal of Infectious Diseases, 217*, 1851–1853.
Khan, N., Vidyarthi, A., Amir, M., Mushtaq, K., & Agrewala, J. N. (2017). T-cell exhaustion in tuberculosis: Pitfalls and prospects. *Critical Reviews in Microbiology, 43*, 133–141.
Kim, C. C., Baccarella, A. M., Bayat, A., Pepper, M., & Fontana, M. F. (2019). Fcrl5(+) memory B cells exhibit robust recall responses. *Cell Reports, 27*, 1446–1460. e4.
Kirkham, C. L., & Carlyle, J. R. (2014). Complexity and diversity of the Nkr-P1:Clr (Klrb1:Clec2) recognition systems. *Frontiers in Immunology, 5*, 214.
Kong, Y., Zhu, L., Schell, T. D., Zhang, J., Claxton, D. F., Ehmann, W. C., Rybka, W. B., George, M. R., Zeng, H., & Zheng, H. (2016). T-cell Immunoglobulin and Itim domain (Tigit) associates with Cd8+ T-cell exhaustion and poor clinical outcome in Aml patients. *Clinical Cancer Research, 22*, 3057–3066.
Korber, B., Muldoon, M., Theiler, J., Gao, F., Gupta, R., Lapedes, A., Hahn, B. H., Wolinsky, S., & Bhattacharya, T. (2000). Timing the ancestor of the Hiv-1 pandemic strains. *Science, 288*, 1789–1796.
Korsunsky, I., Millard, N., Fan, J., Slowikowski, K., Zhang, F., Wei, K., Baglaenko, Y., Brenner, M., Loh, P. R., & Raychaudhuri, S. (2019). Fast, sensitive and accurate integration of single-cell data with Harmony. *Nature Methods, 16*, 1289–1296.
Laguette, N., Sobhian, B., Casartelli, N., Ringeard, M., Chable-Bessia, C., Ségéral, E., Yatim, A., Emiliani, S., Schwartz, O., & Benkirane, M. (2011). Samhd1 is the dendritic- and myeloid-cell-specific Hiv-1 restriction factor counteracted by Vpx. *Nature, 474*, 654–657.
Lastrucci, C., Bénard, A., Balboa, L., Pingris, K., Souriant, S., Poincloux, R., Al Saati, T., Rasolofo, V., González-Montaner, P., Inwentarz, S., Moraña, E. J., Kondova, I., Verreck, F. A., Sasiain Mdel, C., Neyrolles, O., Maridonneau-Parini, I., Lugo-Villarino, G., & Cougoule, C. (2015). Tuberculosis is associated with expansion of a motile, permissive and immunomodulatory Cd16(+) monocyte population via the Il-10/Stat3 axis. *Cell Research, 25*, 1333–1351.
Lawn, S. D., Harries, A. D., Williams, B. G., Chaisson, R. E., Losina, E., De Cock, K. M., & Wood, R. (2011). Antiretroviral therapy and the control of Hiv-associated tuberculosis. Will Art do it? *International Journal of Tuberculosis & Lung Disease, 15*, 571–581.
Lawn, S. D., Pisell, T. L., Hirsch, C. S., Wu, M., Butera, S. T., & Toossi, Z. (2001). Anatomically compartmentalized human immunodeficiency virus replication in Hla-Dr+ cells and Cd14+ macrophages at the site of pleural tuberculosis coinfection. *The Journal of Infectious Diseases, 184*, 1127–1133.
León-Rivera, R., Morsey, B., Niu, M., Fox, H. S., & Berman, J. W. (2020). Interactions of monocytes, Hiv, and art identified by an Innovative scrnaseq pipeline: Pathways to reservoirs and Hiv-associated comorbidities. *MBio, 11*.
León-Rivera, R., Veenstra, M., Donoso, M., Tell, E., Eugenin, E. A., Morgello, S., & Berman, J. W. (2021). Central nervous system (Cns) viral seeding by mature monocytes and potential therapies to reduce Cns viral reservoirs in the cart era. *MBio, 12*.
Liu, R., Gao, Q., Foltz, S. M., Fowles, J. S., Yao, L., Wang, J. T., Cao, S., Sun, H., Wendl, M. C., Sethuraman, S., Weerasinghe, A., Rettig, M. P., Storrs, E. P., Yoon, C. J., Wyczalkowski, M. A., Mcmichael, J. F., Kohnen, D. R., King, J., Goldsmith, S. R., … Ding, L. (2021). Co-evolution of tumor and immune cells during progression of multiple myeloma. *Nature Communications, 12*, 2559.
Liu, C., Wu, T., Fan, F., Liu, Y., Wu, L., Junkin, M., Wang, Z., Yu, Y., Wang, W., & Wei, W. J. B. (2019). *A portable and cost-effective microfluidic system for massively parallel single-cell transcriptome profiling*.
Maertzdorf, J., Mcewen, G., Weiner, J., 3rd, Tian, S., Lader, E., Schriek, U., Mayanja-Kizza, H., Ota, M., Kenneth, J., & Kaufmann, S. H. (2016). Concise gene signature for point-of-care classification of tuberculosis. *EMBO Molecular Medicine, 8*, 86–95.
Mahamed, D., Boulle, M., Ganga, Y., Mc Arthur, C., Skroch, S., Oom, L., Catinas, O., Pillay, K., Naicker, M., Rampersad, S., Mathonsi, C., Hunter, J., Wong, E. B., Suleman, M., Sreejit, G., Pym, A. S., Lustig, G., & Sigal, A. (2017). Intracellular growth of Mycobacterium tuberculosis after macrophage cell death leads to serial killing of host cells. *Elife, 6*.
Marais, B. J., Gie, R. P., Schaaf, H. S., Hesseling, A. C., Obihara, C. C., Starke, J. J., Enarson, D. A., Donald, P. R., & Beyers, N. (2004). The natural history of childhood intra-thoracic tuberculosis: A critical review of literature from the pre-chemotherapy era. *International Journal of Tuberculosis & Lung Disease, 8*, 392–402.
Marais, S., Meintjes, G., Lesosky, M., Wilkinson, K. A., & Wilkinson, R. J. (2016). Interleukin-17 mediated differences in the pathogenesis of Hiv-1-associated tuberculous and cryptococcal meningitis. *AIDS, 30*, 395–404.
Meng, Q., Sayin, I., Canaday, D. H., Mayanja-Kizza, H., Baseke, J., & Toossi, Z. (2016). Immune activation at sites of Hiv/Tb Co-infection contributes to the pathogenesis of Hiv-1 disease. *PLoS One, 11*, Article e0166954.
Monroe, K. M., Yang, Z., Johnson, J. R., Geng, X., Doitsh, G., Krogan, N. J., & Greene, W. C. (2014). Ifi16 Dna sensor is required for death of lymphoid Cd4 T cells abortively infected with Hiv. *Science, 343*, 428–432.
Naing, A., Infante, J. R., Papadopoulos, K. P., Chan, I. H., Shen, C., Ratti, N. P., Rojo, B., Autio, K. A., Wong, D. J., Patel, M. R., Ott, P. A., Falchook, G. S., Pant, S., Hung, A., Pekarek, K. L., Wu, V., Adamow, M., Mccauley, S., Mumm, J. B., … Oft, M. (2018). Pegylated Il-10 (Pegilodecakin) induces systemic immune activation, Cd8(+) T cell invigoration and polyclonal T cell expansion in cancer patients. *Cancer Cell, 34*, 775–791. e3.
Nakata, K., Rom, W. N., Honda, Y., Condos, R., Kanegasaki, S., Cao, Y., & Weiden, M. (1997). Mycobacterium tuberculosis enhances human immunodeficiency virus-1 replication in the lung. *American Journal of Respiratory and Critical Care Medicine, 155*, 996–1003.
Nwimo, I. O., Elom, N. A., Ilo, C. I., Ojide, R. N., Ezugwu, U. A., Eke, V. U., & Ezugwu, L. E. (2020). Hiv/aids knowledge and attitude towards people living with Hiv/Aids (Plwha): A cross-sectional study of primary school teachers. *Journal of African Health Sciences, 20*, 1591–1600. J. A. H. S.
O'garra, A., Redford, P. S., Mcnab, F. W., Bloom, C. I., Wilkinson, R. J., & Berry, M. P. (2013). The immune response in tuberculosis. *Annual Review of Immunology, 31*, 475–527.
Piccioli, D., Tavarini, S., Borgogni, E., Steri, V., Nuti, S., Sammicheli, C., Bardelli, M., Montagna, D., Locatelli, F., & Wack, A. (2007). Functional specialization of human circulating Cd16 and Cd1c myeloid dendritic-cell subsets. *Blood, 109*, 5371–5379.
Pinto, A. K., Daffis, S., Brien, J. D., Gainey, M. D., Yokoyama, W. M., Sheehan, K. C., Murphy, K. M., Schreiber, R. D., & Diamond, M. S. (2011). A temporal role of type I interferon signaling in Cd8+ T cell maturation during acute West Nile virus infection. *PLoS Pathogens, 7*, Article e1002407.
Pizzolato, G., Kaminski, H., Tosolini, M., Franchini, D. M., Pont, F., Martins, F., Valle, C., Labourdette, D., Cadot, S., Quillet-Mary, A., Poupot, M., Laurent, C., Ysebaert, L., Meraviglia, S., Dieli, F., Merville, P., Milpied, P., Déchanet-Merville, J., & Fournié, J. J. (2019). Single-cell Rna sequencing unveils the shared and the distinct cytotoxic hallmarks of human Tcrvδ1 and Tcrvδ2 γδ T lymphocytes. *Proceedings of the National Academy of Sciences of the U S A, 116*, 11906–11915.

Portugal, S., Obeng-Adjei, N., Moir, S., Crompton, P. D., & Pierce, S. K. (2017). Atypical memory B cells in human chronic infectious diseases: An interim report. *Cellular Immunology, 321*, 18–25.

Ramirez, P. W., Famiglietti, M., Sowrirajan, B., Depaula-Silva, A. B., Rodesch, C., Barker, E., Bosque, A., & Planelles, V. (2014). Downmodulation of Ccr7 by Hiv-1 Vpu results in impaired migration and chemotactic signaling within Cd4⁺ T cells. *Cell Reports, 7*, 2019–2030.

Reizis, B. (2010). Regulation of plasmacytoid dendritic cell development. *Current Opinion in Immunology, 22*, 206–211.

Russell, D. G. (2007). Who puts the tubercle in tuberculosis? *Nature Reviews Microbiology, 5*, 39–47.

Sampath, P., Moideen, K., Ranganathan, U. D., & Bethunaickan, R. (2018). Monocyte subsets: Phenotypes and function in tuberculosis infection. *Frontiers in Immunology, 9*, 1726.

Schumann, K., Raju, S. S., Lauber, M., Kolb, S., Shifrut, E., Cortez, J. T., Skartsis, N., Nguyen, V. Q., Woo, J. M., Roth, T. L., Yu, R., Nguyen, M. L. T., Simeonov, D. R., Nguyen, D. N., Targ, S., Gate, R. E., Tang, Q., Bluestone, J. A., Spitzer, M. H., Ye, C. J., & Marson, A. (2020). Functional Crispr dissection of gene networks controlling human regulatory T cell identity. *Nature Immunology, 21*, 1456–1466.

Sharan, R., Bucşan, A. N., Ganatra, S., Paiardini, M., Mohan, M., Mehra, S., Khader, S. A., & Kaushal, D. (2020). Chronic immune activation in Tb/Hiv Co-infection. *Trends in Microbiology, 28*, 619–632.

Shelyakin, P. V., Lupyr, K. R., Egorov, E. S., Kofiadi, I. A., Staroverov, D. B., Kasatskaya, S. A., Kriukova, V. V., Shagina, I. A., Merzlyak, E. M., Nakonechnaya, T. O., Latysheva, E. A., Manto, I. A., Khaitov, M. R., Lukyanov, S. A., Chudakov, D. M., & Britanova, O. V. (2021). Naïve regulatory T cell subset is altered in X-linked Agammaglobulinemia. *Frontiers in Immunology, 12*, 697307.

Singh, S., Toor, J. S., Sharma, A., & Arora, S. K. (2020). Signature genes associated with immunological non-responsiveness to anti-retroviral therapy in Hiv-1 subtype-c infection. *PLoS One, 15*, Article e0234270.

Smith, D. W., Mcmurray, D. N., Wiegeshaus, E. H., Grover, A. A., & Harding, G. E. (1970). Host-parasite relationships in experimental airborne tuberculosis. Iv. Early events in the course of infection in vaccinated and nonvaccinated Guinea pigs. *American Review of Respiratory Disease, 102*, 937–949.

Sonnenberg, P., Glynn, J. R., Fielding, K., Murray, J., Godfrey-Faussett, P., & Shearer, S. (2005). How soon after infection with Hiv does the risk of tuberculosis start to increase? A retrospective cohort study in South African gold miners. *The Journal of Infectious Diseases, 191*, 150–158.

Sullivan, Z. A., Wong, E. B., Ndung'u, T., Kasprowicz, V. O., & Bishai, W. R. (2015). Latent and active tuberculosis infection increase immune activation in individuals Co-infected with Hiv. *EBioMedicine, 2*, 334–340.

Teitell, M. A. (2005). The Tcl1 family of oncoproteins: Co-activators of transformation. *Nature Reviews Cancer, 5*, 640–648.

Thomas, D. A., & Massagué, J. (2005). Tgf-beta directly targets cytotoxic T cell functions during tumor evasion of immune surveillance. *Cancer Cell, 8*, 369–380.

Toossi, Z., Funderburg, N. T., Sirdeshmuk, S., Whalen, C. C., Nanteza, M. W., Johnson, D. F., Mayanja-Kizza, H., & Hirsch, C. S. (2013). Systemic immune activation and microbial translocation in dual Hiv/tuberculosis-infected subjects. *The Journal of Infectious Diseases, 207*, 1841–1849.

Townsley, S. M., Donofrio, G. C., Jian, N., Leggat, D. J., Dussupt, V., Mendez-Rivera, L., Eller, L. A., Cofer, L., Choe, M., Ehrenberg, P. K., Geretz, A., Gift, S., Grande, R., Lee, A., Peterson, C., Piechowiak, M. B., Slike, B. M., Tran, U., Joyce, M. G., … Krebs, S. J. (2021). B cell engagement with Hiv-1 founder virus envelope predicts development of broadly neutralizing antibodies. *Cell Host & Microbe, 29*, 564–578. e9.

Urdahl, K. B., Shafiani, S., & Ernst, J. D. (2011). Initiation and regulation of T-cell responses in tuberculosis. *Mucosal Immunology, 4*, 288–293.

Villani, A. C., Satija, R., Reynolds, G., Sarkizova, S., Shekhar, K., Fletcher, J., Griesbeck, M., Butler, A., Zheng, S., Lazo, S., Jardine, L., Dixon, D., Stephenson, E., Nilsson, E., Grundberg, I., Mcdonald, D., Filby, A., Li, W., De Jager, P. L., … Hacohen, N. (2017). Single-cell Rna-seq reveals new types of human blood dendritic cells, monocytes, and progenitors. *Science, 356*.

Vitale, M., Falco, M., Castriconi, R., Parolini, S., Zambello, R., Semenzato, G., Biassoni, R., Bottino, C., Moretta, L., & Moretta, A. (2001). Identification of Nkp80, a novel triggering molecule expressed by human Nk cells. *European Journal of Immunology, 31*, 233–242.

Wang, S., Zhang, Q., Hui, H., Agrawal, K., Karris, M. A. Y., & Rana, T. M. (2020). An atlas of immune cell exhaustion in Hiv-infected individuals revealed by single-cell transcriptomics. *Emerging Microbes & Infections, 9*, 2333–2347.

Weng, N. P., Araki, Y., & Subedi, K. (2012). The molecular basis of the memory T cell response: Differential gene expression and its epigenetic regulation. *Nature Reviews Immunology, 12*, 306–315.

World Health Organization. (2020). *Global tuberculosis report 2020*.

Yu, G., Wang, L. G., Han, Y., & He, Q. Y. (2012). clusterprofiler: an R package for comparing biological themes among gene clusters. *Omics, 16*, 284–287.

Zeng, M., Southern, P. J., Reilly, C. S., Beilman, G. J., Chipman, J. G., Schacker, T. W., & Haase, A. T. (2012). Lymphoid tissue damage in Hiv-1 infection depletes naïve T cells and limits T cell reconstitution after antiretroviral therapy. *PLoS Pathogens, 8*, Article e1002437.

Zhang, W., Shi, L., Zhao, Z., Du, P., Ye, X., Li, D., Cai, Z., Han, J., & Cai, J. (2019). Disruption of Ctla-4 expression on peripheral blood Cd8+Tcell enhances anti -tumor efficacy in bladder cancer. *Cancer Chemotherapy and Pharmacology, 83*, 911–920.

Zheng, Q., Xu, J., Gu, X., Wu, F., Deng, J., Cai, X., Wang, G., Li, G., & Chen, Z. (2020). Immune checkpoint targeting Tigit in hepatocellular carcinoma. *American Journal of Translational Research, 12*, 3212–3224.

Zhu, T., Muthui, D., Holte, S., Nickle, D., Feng, F., Brodie, S., Hwangbo, Y., Mullins, J. I., & Corey, L. (2002). Evidence for human immunodeficiency virus type 1 replication in vivo in Cd14(+) monocytes and its potential role as a source of virus in patients on highly active antiretroviral therapy. *Journal of Virology, 76*, 707–716.

Zhu, L., Yang, P., Zhao, Y., Zhuang, Z., Wang, Z., Song, R., Zhang, J., Liu, C., Gao, Q., Xu, Q., Wei, X., Sun, H. X., Ye, B., Wu, Y., Zhang, N., Lei, G., Yu, L., Yan, J., Diao, G., … Liu, W. J. (2020). Single-cell sequencing of peripheral mononuclear cells reveals distinct immune response landscapes of Covid-19 and influenza patients. *Immunity, 53*, 685–696. e3.